International Journal of Medical Physics, Clinical Engineering and Radiation Oncology, 2017, 6, 323-335
http://www.scirp.org/journal/ijmpcero
ISSN Online: 2168-5444
ISSN Print: 2168-5436

Accuracy Comparison of 4D Computed Tomography (4DCT) and 4D Cone Beam Computed Tomography (4DCBCT)

Tzu-Cheng Lee[1], Stephen R. Bowen[2,3], Sara St. James[2*], George A. Sandison[2,3], Paul E. Kinahan[1,2,3*], Matthew J. Nyflot[2,3*]

[1]Department of Bioengineering, University of Washington, Seattle, WA, USA
[2]Department of Radiation Oncology, University of Washington, Seattle, WA, USA
[3]Department of Radiology, University of Washington, Seattle, WA, USA
Email: *nyflot@uw.edu

How to cite this paper: Lee, T.-C., Bowen, S.R., St. James, S., Sandison, G.A., Kinahan, P.E. and Nyflot, M.J. (2017) Accuracy Comparison of 4D Computed Tomography (4DCT) and 4D Cone Beam Computed Tomography (4DCBCT). *International Journal of Medical Physics, Clinical Engineering and Radiation Oncology*, **6**, 323-335.
https://doi.org/10.4236/ijmpcero.2017.63029

Received: July 25, 2017
Accepted: August 27, 2017
Published: August 30, 2017

Abstract

The ability of respiratory-correlated fan beam CT (4DCT) and respiratory-correlated cone beam CT (4DCBCT) to accurately estimate tumor volume is critical to accurate dosimetry and treatment verification for lung stereotactic body radiation therapy (SBRT) and other motion-managed therapies. However, it is known that 4DCT and 4DCBCT differ in aspects of image acquisition and reconstruction that may lead to discrepancies between the two modalities. To evaluate quantitative differences between 4DCT and 4DCBCT imaging under respiratory motion, we performed a phantom study in the ground truth setting. A programmable respiratory motion phantom was used to simulate the 1D S-I position of a known-size lesion. Ten sinusoidal and twenty patient-specific breathing waveforms were applied to drive lesion motion during the 4DCT and 4DCBCT acquisitions. The difference in lesion volume acquired between the two imaging modalities was as high as 34.4% and 18.4% for sinusoidal and patient-specific breathing motions, respectively. When compared to the true volume, 4DCT measurement often underestimated the lesion size whereas 4DCBCT overestimated the lesion volume in most of the cases. 4DCBCT gave more accurate recovery of the volume than 4DCT for most settings tested in this study. These findings may be helpful for improving the definition of internal target and planning target volume margins, and extracting quantitative information from on-board treatment verification imaging.

Keywords

4DCT, 4DCBCT, Verification Imaging, Respiratory Motion Phantom

1. Introduction

Accurate computed tomography (CT) studies under the presence of respiratory motion are necessary for treatment planning, treatment verification, and adaptive radiotherapy in many cancers, most commonly for cancers of the lung, liver, and abdomen [1] [2] [3] [4] [5]. 4DCT imaging may be used for respiratory motion assessment and creating an external beam radiation treatment plan for a free-breathing patient [6] [7]. Radiotherapy image-guided verification is commonly performed by comparing lesion position and motion estimated in the treatment room with cone beam CT (CBCT), CT on rails, megavoltage CT (MVCT) or other methods to the primary planning CT study acquired at the time of treatment simulation. Beyond the critical role of verification imaging in patient setup, changes in CT volumes have been used as indications for adaptive re-planning and modeled to extract radiobiological parameters [8] [9].

It is known that respiratory motion leads to significant imaging artifacts which may lead to incorrect treatment planning volumes, lesion localization, or inference of change in tumor volume over time. Respiratory-correlated computed tomography (4DCT) using external respiratory surrogates was first proposed as solution for this problem [10] [11] [12] [13] and has rapidly become a standard of care for radiotherapy simulation in the presence of respiratory motion [14] [15]. In the intervening years, cone beam computed tomography (CBCT) technology has proliferated on linear accelerators to provide image guidance for radiotherapy verification, and recently, respiratory-correlated cone beam CT (4DCBCT) has become clinically available [16] [17] [18]. Sonke *et al.* investigated 4DCBCT versus 3DCBCT and fluoroscopy and found motion artifacts in 4D dataset were substantially reduced compared to a 3D scan [17]. Sweeney *et al.* investigated inter-observer variability of target localization for 4DCBCT and 3DCBCT imaging with patient data and found significantly reduced variability with 4DCBCT [19]. Lee *et al.* and Iramina *et al.* further examined the impact of scanning parameters and motion sorting methods related to the accuracy of 4DCBCT images [20] [21].

However, clinical investigation of comparisons of 4DCBCT and 4DCT imaging for tumor motion assessment has indicated significant differences in some patients [22]. 4DCT and 4DCBCT imaging differs in numerous aspects in terms of image acquisition, hardware geometry, and binning techniques [23] [24]. These differences include smaller x-ray beam volumetric coverage in CT versus much larger coverage in CBCT for a single rotation, scan time on the order of seconds in 4DCT versus minutes in 4DCBCT, arc detector versus flat panel detector geometry employed with different anti-scatter setups, and external surrogates in 4DCT versus internal tracking in 4DCBCT of respiratory motion. To date, investigations of accuracy of respiratory-correlated fan beam versus cone beam CT imaging in the presence of respiratory motion in the ground truth setting have been limited. Researchers have compared 3DCBCT image to the 4DCT maximum intensity projection (MIP) reconstructed image of anthropomorphic respiratory phantoms and found contradictory results [25] [26]. Nevertheless,

the relative accuracy of 4DCBCT and 4DCT in the ground truth setting is unknown.

We had shown the uptake accuracy in 4D phased-match CT attenuation corrected 4DPET could be significantly compromised due to patient's irregular breathing pattern and the nature of acquisition time difference between two modalities [27]. In this work, we will focus on the impact of respiratory motion on CT acquisition by comparing the accuracy of 4DCT and 4DCBCT in the ground truth setting with an anthropomorphic respiratory phantom. These results may be informative for treatment planning, treatment verification, longitudinal response assessment, and adaptive radiotherapy for thoracic and abdominal cancers.

2. Methods

2.1. Anthropomorphic Phantom

The Quasar programmable respiratory motion phantom (Modus Medical Devices Inc., ON, Canada) was used for this study. A custom insert was designed, consisting of a water-filled 24 mm outer-diameter sphere simulating a lung lesion, surrounded by polystyrene pellets comparable to the density of lung. The Quasar phantom has a mount for an infrared marker which moves at a 1:1 ratio to the phantom insert. The motion of the infrared marker was captured with an RPM camera (RPM, Varian Medical Systems, Palo Alto, CA). An image of the phantom is shown in Figure 1. The motion of the Quasar phantom is one dimensional (superior-inferior) and can be programmed using sinusoidal breathing traces or representative patient traces distributed with the phantom.

2.2. Phantom Motion

To evaluate the fidelity of the 4DCT and 4DCBCT studies, the water sphere was driven by 10 sinusoidal respiratory waveforms (period 3, 4, 5, 6, 7 seconds, 15 and 30 mm amplitude) and 20 patient-derived respiratory waveforms provided by the Quasar software (10 patient waveforms with period 4.2 ± 0.7 - 6.6 ± 1.6 seconds, nominal 15 and 30 mm peak-to-peak amplitude, mean 9.9 ± 1.2 - 19.8 ± 2.3 mm amplitude). It should be noted that the patient-specific respiratory

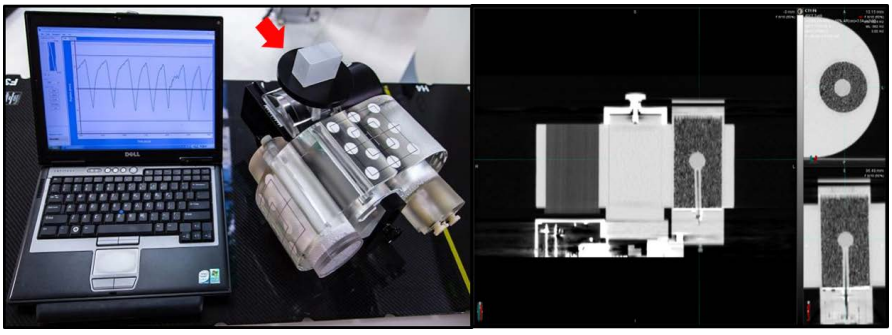

Figure 1. On left, programmable respiratory phantom with custom anthropomorphic insert. The mount for the infrared marker cubic is indicated with a red arrow. On right, representative CT slice of phantom geometry.

waveforms are denoted by their nominal peak to peak amplitudes, however, the mean amplitudes are less in magnitude due to baseline drift in respiration.

2.3. CT Studies

Reference images were acquired of the phantom under static conditions for both CT and CBCT studies. A helical CT scan was acquired using a GE LightSpeed RT16 CT scanner (GE Healthcare, Waukesha, WI). Scan parameters were 120 kVp, 320 mAs, 2.5 mm slice thickness, 1.375 pitch factor. For CBCT, the static phantom case was acquired using the Chest M20 F1 preset in Elekta XVI (X-ray Volume Imaging ver.4.5, Elekta, Stockholm, Sweden). Scan parameters were 120 kVp, M20 medium offset field of view with F1 bowtie filter, 40 mA, 40 ms, 660 projections. The water sphere was contoured using threshold segmentation in MIM 6.2.5 (MIM Software, Cleveland, OH) using the known volume of the sphere as ground truth to define segmentation settings. The sphere has a stem which is used to fill the sphere with water; this stem was manually excluded from the contoured volume.

Then, 4DCT and 4DCBCT images were acquired for each motion case, resulting in 30 4D imaging studies (10 sinusoidal, 20 patient-derived). For the 4DCT studies, the cine duration was set as the breathing period plus 1 second. The duration between cine images was set as the respiratory period in seconds divided by 10. All cine CT images were acquired at 120 kVp, 8 mAs, with the same voxel size used in the static study (0.977 mm × 0.977 mm × 2.5 mm). All 4DCBCT images were acquired with the Symmetry 4D preset on an Elekta Synergy linear accelerator with M20 field of view, F1 bowtie filter, 120 kVp tube voltage, 20 mA tube current, and 16 ms x-ray pulse length. 1320 projections were acquired over a 360-degree gantry rotation for one CBCT scan.

4DCT studies were phase-sorted into 10 phase images in Advantage 4D. The 4DCBCT studies were reconstructed in the XVI software suite, in ten phases at 128 × 205 × 205 voxels and 2.0 × 2.0 × 2.0 mm/voxel. At the time of data analysis, DICOM export of 4DCBCT data was not possible from the XVI software. Native format 4DCBCT images were reduced in dimensionality from raw 4D data to 10 3D matrices representing individual image phases in ANALYZE format (Biomedical Imaging Resource, Mayo Foundation, Rochester, MN) with VV, a 4D Slicer [28]. Images were then batch converted from ANALYZE to DICOM in AMIDE [29]. 4DCT and 4DCBCT DICOM images were imported into MIM 6.2.5 for image analysis. Object volumes were defined on CT and CBCT images via threshold segmentation, applying the identical threshold as used for the static imaging task. Contours were visually assessed for conformality.

The water sphere was contoured on individual phase images via threshold segmentation on every 4D study. In total 300 4DCT and 300 4DCBCT phase images were analyzed. Differences in the water sphere volumes (compared to the reference volumes) were evaluated. The averages across studies were evaluated, along with the volumes as a function of the phase.

3. Results

3.1. Segmented Volume Bias for 4DCT and 4DCBCT Imaging

Representative 4DCT and 4DCBCT images are shown in Figure 2. The tabulated percent differences between segmented volumes under motion and the reference volume are shown for 4DCT and 4DCBCT images in Table 1.

The threshold segmentation of the water sphere resulted in a volume of 7.65 mL, 6% greater than the calculated volume of 7.28 mL. With sinusoidal motion of amplitude 15 mm, the threshold volume of the water sphere was found to be underestimated at 6.69 ± 0.82 mL using 4DCT, compared to an overestimation of similar magnitude of 8.28 ± 0.28 mL using 4DCBCT. However, when the amplitude was increased to 30 mm, the magnitude of underestimation was greater for 4DCT at 5.58 ± 1.36 mL, while average volumes measured by 4DCBCT were not greatly changed at 8.21 ± 0.23 mL. Furthermore 4DCBCT volumes were characterized by greater variability over the sinusoidal dataset as measured by standard deviation.

For the patient-derived waveforms of amplitude 15 mm, trends were similar to the sinusoidal case. The threshold volume of the water sphere was found to be 7.16 ± 0.60 mL using 4DCT, compared to 8.16 ± 0.16 mL using 4DCBCT. Again, when the amplitude of the waveforms was increased to 30 mm, greater change in the average volume of the water sphere was found with 4DCT (6.51 ± 1.51 mL), compared to 7.92 ± 0.26 mL using 4DCBCT. Three of 20 4DCT patient waveforms, all 15 mm peak-to-peak amplitude with irregular respiration, could not be phase-sorted in Advantage 4D and were excluded from analysis. All 4DCBCT images sets could be phase sorted.

Over all studies, the volumes from the 4DCBCT studies were more accurate

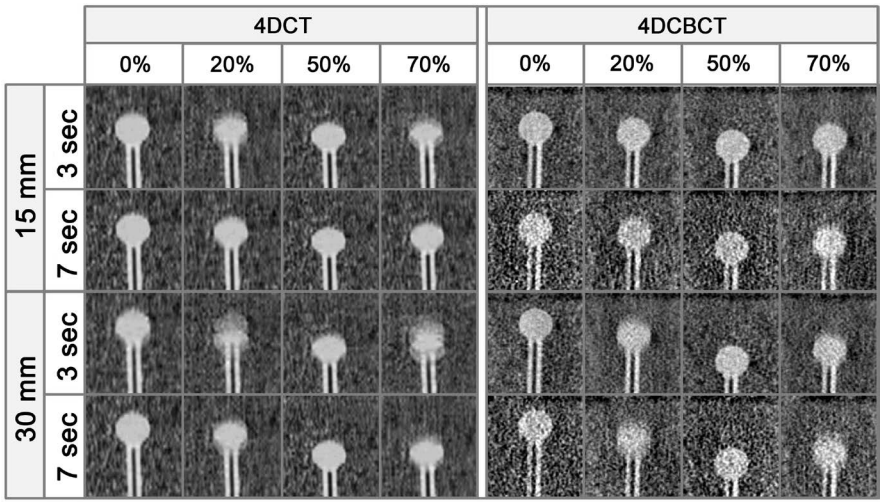

Figure 2. Representative 4DCT and 4DCBCT phase images for inhale (0%), exhale (50%), and intermediate (20%, 70%) respiratory phases. For respiratory conditions which correspond to high velocity (low period) or high amplitude, 4DCT images exhibit phase-specific image quality characterized by artifacting and motion blur at intermediate phases. While 4DCBCT images are characterized by increased noise, minimal artifacting at intermediate phases and greatly reduced variability between image phases is seen.

than volumes defined on 4DCT images for all motion cases except for the nominal 15 mm patient-specific traces. For sinusoidal waveforms with 30 mm peak-to-peak amplitude, 4DCT image measurements underestimated lesion volume by 27.1% on average (5.54 ± 1.36 mm, range 1.53 - 7.42 mm). Images segmented on 4DCBCT were more accurate, overestimating lesion volume by 7.3% on average (8.21 ± 0.23, range 7.27 - 8.56). Similar results were seen for sinusoidal waveforms with 15 mm peak-to-peak amplitude and patient waveforms with 30 mm nominal: images segmented on 4DCT average underestimated lesion volume by 12.8% and 14.9% on average while images segmented on 4DCBCT were more accurate, overestimating lesion volume by 8.0% and 3.5% on average. For the patient waveforms with 15 mm nominal amplitude the trends reversed, with 4DCT underestimating by 6.4% and 4DCBCT overestimating by 6.7%. In this scenario, it should be noted that the 4DCT data set was smaller than the 4DCBCT data set as three patient traces could not be used for 4D reconstruction as noted in the results section. For all studies, the accuracy was proportional to respiratory amplitude, with greater amplitudes resulting in lower accuracy.

3.2. Segmented Volume for 4DCT and 4DCBCT Imaging as a Function of Respiratory Waveform and Phase

Graphs depicting accuracy of 4DCT and 4DCBCT imaging as a function of respiratory waveform and image phase are depicted in **Figure 3**.

When evaluating 4DCT images of sinusoidal waveforms as a function of respiratory period, segmented volumes showed reduced accuracy (smaller volumes) with shorter periods (greater velocity). This was observed for the 30 mm amplitude traces, likely due to the fact that greater amplitudes result in greater sphere velocities. For 15 mm sine waveforms, volume recovery appeared to reach a threshold at periods of approximately 5 - 6 seconds, above which no benefit was achieved. For 30 mm sine waveforms, no threshold was reached over the range of periods studied (3 - 7 s). 4DCBCT images showed trends in the opposite direction where longer periods corresponded to smaller volumes, though this trend was smaller in magnitude than that observed for 4DCT imaging.

The variability of volume measured over all 4DCT image phases was large (range 1.50 - 10.96 mL). Specifically, image phases corresponding to end-inhale and end-exhale phases of the respiratory cycle (0% max. inspiration and 50% max. inspiration) were more accurate than phases corresponding to intermediate portions of the respiratory cycle (*see* **Table 1**), with this effect being larger for 30 mm sine waveforms than 15 mm sine waveforms. However, volumetric differences from only end-phase imaging between two modalities were still prominent in all combinations of waveform and amplitude (13.2% 16.4%, 12.4%, and 15.9% for 15-mm sinusoid, 30-mm sinusoid, 15-mm patient waveform, and 30-mm patient waveforms, respectively). Differences were not found between end phases and intermediate phases for 4DCBCT imaging.

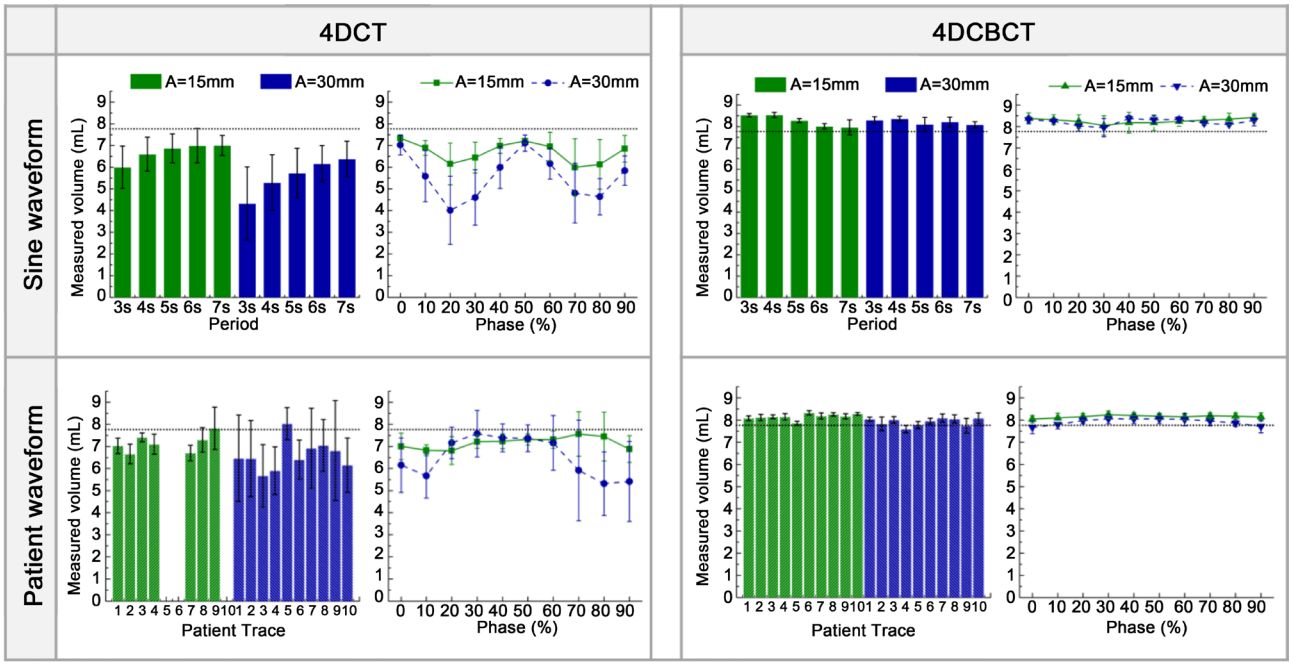

Figure 3. Segmented volume for 4DCT and 4DCBCT imaging as a function of respiratory waveform and phase. For sinusoidal motion, 4DCT exhibits period-dependent trends where volume recovery decreases with shorter period (greater velocity). Additionally, 4DCT imaging demonstrates phase-dependent trends where volume recovery decreases at intermediate respiratory phases. For patient-specific respiratory motion, phase-specific trends are less pronounced but greatest accuracy is still seen at end-exhale phases. Three waveforms could not be reconstructed in Advantage 4D and were excluded. No strong trends as a function of respiratory waveform or phase are observed for CBCT imaging. Dashed line indicates reference volume.

Table 1. Segmented volume and percent difference relative to the reference volume as a function of imaging modality, respiratory waveform, and motion amplitude. End-phase volume and difference represent the matrices measured with only maximum inspiration and expiration phases.

Control Volume 7.65 ml	Nominal Amplitude (mm)	Mean Amplitude (mm)	4DCT				4DCBCT			
			Volume (mL)	Difference (%)	End-phase Volume (mL)	End-phase Difference (%)	Volume (mL)	Difference (%)	End-phase Volume (mL)	End-phase Difference (%)
Sinusoid	15	15	6.69 ± 0.82	**−12.8**	7.27 ± 0.14	**−5.0**	8.28 ± 0.28	**8.0**	8.28 ± 0.32	**8.2**
	30	30	5.54 ± 1.36	**−27.1**	7.07 ± 0.40	**−7.6**	8.21 ± 0.23	**7.3**	8.32 ± 0.16	**8.8**
Patient waveforms	15	9.90 ± 1.17	7.16 ± 0.60	**−6.4**	7.16 ± 0.44	**−6.4**	8.16 ± 0.16	**6.7**	8.11 ± 0.16	**6.0**
	30	19.80 ± 2.34	6.51 ± 1.51	**−14.9**	6.76 ± 1.13	**−11.6**	7.92 ± 0.26	**3.5**	7.98 ± 0.18	**4.3**

4. Discussion

4DCT and 4DCBCT are routinely used in external beam radiation therapy, with 4DCT used at the time of patient simulation and treatment planning and 4DCBCT used at the time of patient treatment. The volume, shape, and position of these two studies are often compared, with the assumption that the differences between the studies are only related to the image quality (e.g. noise, HU bias, spatial resolution) and that volumetric differences are due to anatomic differences alone (e.g. tumor progression or response to therapy). We investigated the volume accuracy and difference of 4DCT and 4DCBCT imaging under the

common clinical settings in the ground truth setting with a respiratory phantom. We found that systematic volume differences could be observed where no volume differences should exist in both sinusoid and patient scans, and 4DCBCT measurement was closer to the truth in most of cases. These volumetric differences between two modalities could be mitigated to a certain extent by choosing end-inhale and end-exhale phases to compare (where the lesion velocity is minimized) and by understanding where discrepancies in volume increase (large amplitude breaths, short breathing cycle). These findings have implications for clinical practice, including verification that treatment planning margins sufficiently encompass tumor motion, construction of maximum intensity and average intensity projections for treatment planning, assessment of longitudinal dose accumulation, or decision to adaptively re-plan based on CBCT imaging.

While both imaging modalities produced artifacts that limited their accuracy, 4DCBCT yielded image-defined target volumes closer to ground truth than 4DCT for all but one of the scenarios tested (15 mm amplitude, patient-derived waveforms). While the use of broad x-ray beams and flat panel detectors inherent to CBCT has led to criticism of image quality due to artifacts caused by scatter and differences in x-ray energy spectrum across the panel, this technology appears well-suited for motion assessment. The modest overestimation of imaging volume was likely due to motion blur, as subjectively 4DCBCT can contain motion blurring artifacts while 4DCT is seen to "freeze" object motion, as well as greater scatter with the broad beam geometry. Beyond lower overall accuracy for 4DCT imaging, object volume measured on the individual phases of the 4DCT varied widely, with the most accurate volume definition being end phases, where the sphere velocity was minimized. Results suggest that 4DCT simulation may underestimate tumor motion, especially in patients with large motion amplitudes.

One limitation of our study is that the respiratory phantom used to simulate the lesion movement had motion only in the S-I direction and respiratory motion naturally occurs in three dimensions. Our finding of inaccuracy in intermediate respiratory phases might lead to greater motion discrepancies in the common case of "c-shaped" respiratory motion. Although we showed the measured volumes between two modalities could also be very different in patient-waveform scans, even if end-phase volume measurements were only phases to be considered, other important measurements related to the image-guided radiation treatment (IGRT) process like the bias of tumor motion between CT and CBCT are not reported here because it could not be fairly evaluated with our 1-D phantom motion setup. Previous studies have reported on similar differences in respiratory motion in patients; e.g. Purdie *et al.* [22] reported that two out of twelve patients showed significant tumor motion differences (distance between end-inhale and end-exhale phases of tumor position) between 4DCT and 4DCBCT measurements.

The difference in 4DCT and 4DCBCT can be explained in part through the physics of image acquisition, notably differences in cone-angle coverage and in

acquisition time. While CBCT images were acquired with a large flat-panel detector, CT images were acquired with a regular 16-row detector (around 2.0 cm in z-direction). The consequence of this is that tumor motion is in the imaging field of view for the entire acquisition for CBCT imaging, but only for several image slices for the CT acquisition. Additionally, the tumor is in the imaging field of view for a shorter period of time for 4DCT (~5 - 10 sec vs. 3.5 - 4 min in 4DCBCT) which may cause bias in patients with irregular respiratory motion because only a small portion of the breathing motion range was covered during the short CT scan [27] [30] [31]. Another challenge is that threshold segmentation settings of ROI were defined on static CT acquisitions. Threshold segmentation has known limitations with reproducibility across scanners and acquisition settings. In this study acquisition-specific threshold settings were determined from the ground truth case. However, for the 4DCT scan, image noise and HU bias are expected to be higher in the low-dose cine acquisition than the helical scan. For CBCT, there were differences in mAs and acquired projections between the 3D and 4D scan. We chose the default manufacturer acquisition profiles for these scans because CBCT parameters are not routinely changed by Elekta XVI users. However, discrepancies in image noise due to photon starvation could be confounding factors in measuring the volume.

The above limitations in terms of image quality imply that conventional protocols used in the 4DCT and 4DCBCT imaging process may not be able to reflect the true anatomic differences from tumor progression or treatment response at this time. To address these challenges, a large body of research is being performed to improve image accuracy under respiratory motion. For 4DCT, optimized low-dose CT protocols [32] [33] [34] [35], scatter corrections [36] [37], approaches regarding the acquisition time [30], motion modeling [38], and more advanced motion gating techniques [39] [40] [41] are being investigated. For 4DCBCT, reconstruction and motion binning techniques [42] [43] are being developed. Evaluating improvements from these methods so that the lesion volume under the respiratory motion can be more accurately estimated by both 4DCT and 4DCBCT is a direction for future work.

5. Conclusion

Respiratory-correlated CT and CBCT imaging is critical for radiation treatment in thoracic cancers. In this study using a dynamic respiratory motion phantom to study the accuracy of 4DCT and 4DCBCT imaging in the ground truth setting, some advantages were seen in both modalities, but 4DCBCT images were generally more accurate and reproducible than those measurements derived from 4DCT images due to the reduced presence of respiratory motion artifacts. These results may be relevant to radiation oncology in the areas of target volume definition, verification imaging, longitudinal response assessment, and adaptive re-planning.

Acknowledgement

Supported in part by NIH grant R01 CA160253.

References

[1] Mageras, G.S., Pevsner, A., Yorke, E.D., Rosenzweig, K.E., Ford, E.C., Hertanto, A., Larson, S.M., Lovelock, D.M., Erdi, Y.E., Nehmeh, S.A., Humm, J.L., and Ling, C.C. (2004) Measurement of Lung Tumor Motion Using Respiration-Correlated CT. *International Journal of Radiation Oncology Biology Physics*, **60**, 933-941.

[2] Shirato, H., Seppenwoolde, Y., Kitamura, K., Onimura, R., and Shimizu, S. (2004) Intrafractional Tumor Motion: Lung and Liver. *Seminars in Radiation Oncology*, **14**, 10-18. https://doi.org/10.1053/j.semradonc.2003.10.008

[3] Goerres, G.W., Burger, C., Kamel, E., Seifert, B., Kaim, A.H., Buck, A., Buehler, T. C., and Von Schulthess, G.K. (2003) Respiration-Induced Attenuation Artifact at PET/CT: Technical Considerations. *Radiology*, **226**, 906-910.

[4] Pan, T., Mawlawi, O., Nehmeh, S.A., Erdi, Y.E., Luo, D., Liu, H.H., Castillo, R., Mohan, R., Liao, Z. and Macapinlac, H.A. (2005) Attenuation Correction of PET Images with Respiration-Averaged CT Images in PET/CT. *Journal of Nuclear Medicine*, **46**, 1481-1487.

[5] Beyer, T., Antoch, G., Blodgett, T., Freudenberg, L.F., Akhurst, T. and Mueller, S. (2003) Dual-Modality PET/CT Imaging: The Effect of Respiratory Motion on Combined Image Quality in Clinical Oncology. *European Journal of Nuclear Medicine and Molecular Imaging*, **30**, 588-596. https://doi.org/10.1007/s00259-002-1097-6

[6] Keall, P. (2004) 4-Dimensional Computed Tomography Imaging and Treatment Planning. *Seminars in Radiation Oncology*, **14**, 81-90. https://doi.org/10.1053/j.semradonc.2003.10.006

[7] Rietzel, E., Chen, G., Choi, N.C. and Willet, C.G. (2005) Four-Dimensional Image-Based Treatment Planning: Target Volume Segmentation and Dose Calculation in the Presence of Respiratory Motion. *International Journal of Radiation Oncology Biology Physics*, **61**, 1535-1550.

[8] Therasse, P., Arbuck, S.G., Eisenhauer, E.A., Wanders, J., Kaplan, R.S., Rubinstein, L., Verweij, J., Van Glabbeke, M., van Oosterom, A.T., Christian, M.C. and Gwyther, S.G. (2000) New Guidelines to Evaluate the Response to Treatment in Solid Tumors. *Journal of the National Cancer Institute*, **92**, 205-216. https://doi.org/10.1093/jnci/92.3.205

[9] Greco, C., Rosenzweig, K., Cascini, G.L. and Tamburrini, O. (2007) Current Status of PET/CT for Tumour Volume Definition in Radiotherapy Treatment Planning for Non-Small Cell Lung Cancer (NSCLC). *Lung Cancer*, **57**, 125-134. https://doi.org/10.1016/j.lungcan.2007.03.020

[10] Ford, E.C., Mageras, G.S., Yorke, E. and Ling, C.C. (2003) Respiration-Correlated Spiral CT: A Method of Measuring Respiratory-Induced Anatomic Motion for Radiation Treatment Planning. *Medical Physics*, **30**, 88-97. https://doi.org/10.1118/1.1531177

[11] Low, D.A., Nystrom, M., Kalinin, E., Parikh, P., Dempsey, J.F., Bradley, J.D., Mutic, S., Wahab, S.H., Islam, T., Christensen, G., Politte, D.G. and Whiting, B.R. (2003) A Method for the Reconstruction of Four-Dimensional Synchronized CT Scans Acquired during Free Breathing. *Medical Physics*, **30**, 1254-1263. https://doi.org/10.1118/1.1576230

[12] Vedam, S.S., Keall, P.J., Kini, V.R., Mostafavi, H., Shukla, H.P. and Mohan, R. (2003) Acquiring a Four-Dimensional Computed Tomography Dataset Using an External Respiratory Signal. *Physics in Medicine & Biology*, **48**, 45-62. https://doi.org/10.1088/0031-9155/48/1/304

[13] Pan, T., Lee, T.-Y., Rietzel, E. and Chen, G.T.Y. (2004) 4D-CT Imaging of a Volume Influenced by Respiratory Motion on Multi-Slice CT. *Medical Physics*, **31**, 333-340. https://doi.org/10.1118/1.1639993

[14] Underberg, R., Lagerwaard, F.J., Cuijpers, J.P., Slotman, B.J., de Koste, J. and Senan, S. (2004) Four-Dimensional CT Scans for Treatment Planning in Stereotactic Radiotherapy for Stage I Lung Cancer. *International Journal of Radiation Oncology Biology Physics*, **60**, 1283-1290. https://doi.org/10.1016/j.ijrobp.2004.07.665

[15] Rietzel, E., Liu, A.K., Doppke, K.P., Wolfgang, J.A., Chen, A.B., Chen, G.T.Y. and Choi, N.C. (2006) Design of 4D Treatment Planning Target Volumes. *International Journal of Radiation Oncology Biology Physics*, **66**, 287-295. https://doi.org/10.1016/j.ijrobp.2006.05.024

[16] Kriminski, S., Mitschke, M., Sorensen, S., Wink, N.M., Chow, P.E., Tenn, S. and Solberg, T.D. (2005) Respiratory Correlated Cone-Beam Computed Tomography on an Isocentric C-Arm. *Physics in Medicine & Biology*, **50**, 5263-5280. https://doi.org/10.1088/0031-9155/50/22/004

[17] Sonke, J.-J., Zijp, L., Remeijer, P. and van Herk, M. (2005) Respiratory Correlated Cone Beam CT. *Medical Physics*, **32**, 1176-1186. https://doi.org/10.1118/1.1869074

[18] Dietrich, L., Jetter, S., Tücking, T., Nill, S. and Oelfke, U. (2006) Linac-Integrated 4D Cone Beam CT: First Experimental Results. *Physics in Medicine & Biology*, **51**, 2939-2952. https://doi.org/10.1088/0031-9155/51/11/017

[19] Sweeney, R.A., Seubert, B., Stark, S., Homann, V., Müller, G., Flentje, M. and Guckenberger, M. (2012) Accuracy and Inter-Observer Variability of 3D versus 4D Cone-Beam CT Based Image-Guidance in SBRT for Lung Tumors. *Radiation Oncology*, **7**, 81. https://doi.org/10.1186/1748-717X-7-81

[20] Lee, S., Yan, G., Lu, B., Kahler, D., Li, J.G. and Sanjiv, S.S. (2015) Impact of Scanning Parameters and Breathing Patterns on Image Quality and Accuracy of Tumor Motion Reconstruction in 4D CBCT: A Phantom Study. *Journal of Applied Clinical Medical Physics*, **16**, 195-212. https://doi.org/10.1120/jacmp.v16i6.5620

[21] Iramina, H., Nakamura, M., Iizuka, Y., Mitsuyoshi, T., Matsuo, Y., Mizowaki, T., Hiraoka, M. and Kanno, I. (2016) The Accuracy of Extracted Target Motion Trajectories in Four-Dimensional Cone-Beam Computed Tomography for Lung Cancer Patients. *Radiotherapy and Oncology*, **121**, 46-51. https://doi.org/10.1016/j.radonc.2016.07.022

[22] Purdie, T.G., Moseley, D.J., Bissonnette, J.-P., Sharpe, M.B., Franks, K., Bezjak, A. and Jaffray, D.A. (2006) Respiration Correlated Cone-Beam Computed Tomography and 4DCT for Evaluating Target Motion in Stereotactic Lung Radiation Therapy. *Acta Oncologica*, **45**, 915-922. https://doi.org/10.1080/02841860600907345

[23] Gupta, R., Cheung, A.C., Bartling, S.H., Lisauskas, J., Grasruck, M., Leidecker, C., Schmidt, B., Flohr, T. and Brady, T.J. (2008) Flat-Panel Volume CT: Fundamental Principles, Technology, and Applications. *RadioGraphics*, **28**, 2009-2022. https://doi.org/10.1148/rg.287085004

[24] Orth, R.C., Wallace, M.J., Kuo, M.D. and Int, T.A.C.S. (2008) C-Arm Cone-Beam CT: General Principles and Technical Considerations for Use in Interventional Radiology. *Journal of Vascular and Interventional Radiology*, **19**, 814-820. https://doi.org/10.1016/j.jvir.2008.02.002

[25] Clements, N., Kron, T., Franich, R., Dunn, L., Roxby, P., Aarons, Y., Chesson, B., Siva, S., Duplan, D. and Ball, D. (2013) The Effect of Irregular Breathing Patterns on Internal Target Volumes in Four-Dimensional CT and Cone-Beam CT Images in the Context of Stereotactic Lung Radiotherapy. *Medical Physics*, **40**, Article ID: 021904. https://doi.org/10.1118/1.4773310

[26] Wang, L., Chen, X., Lin, M.-H., Xue, J., Lin, T., Fan, J., Jin, L. and Ma, C.M. (2013) Evaluation of the Cone Beam CT for Internal Target Volume Localization in Lung Stereotactic Radiotherapy in Comparison with 4D MIP Images. *Medical Physics*, **40**, Article ID: 111709. https://doi.org/10.1118/1.4823785

[27] Nyflot, M.J., Lee, T.-C., Alessio, A.M., Wollenweber, S.D., Stearns, C.W., Bowen, S.R. and Kinahan, P.E. (2015) Impact of CT Attenuation Correction Method on Quantitative Respiratory-Correlated (4D) PET/CT Imaging. *Medical Physics*, **42**, 110. https://doi.org/10.1118/1.4903282

[28] Rit, S., Pinho, R., Delmon, V. and Pech, M. (2011) VV, a 4D Slicer. *Proceedings of the Fourth International Workshop on Pulmonary Image Analysis*, Toronto, 2011, 171-175.

[29] Loening, A.M. and Gambhir, S.S. (2003) AMIDE: A Free Software Tool for Multimodality Medical Image Analysis. *Molecular Imaging*, **2**, 131-137. https://doi.org/10.1162/153535003322556877

[30] Zhang, R., Alessio, A.M., Pierce, L.A., Byrd, D.W., Lee, T.-C., De Man, B. and Kinahan, P.E. (2017) Improved Attenuation Correction for Respiratory Gated PET/CT with Extended-Duration Cine CT: A Simulation Study. *SPIE Medical Imaging*, Orlando, FL, 9 March 2017, Article ID: 10132.

[31] Kinahan, P., Wollenweber, S., Alessio, A., Kohlmyer, S., MacDonald, L., Lewellen, T. and Ganin, A. (2007) Impact of Respiration Variability on Respiratory Gated Whole-Body PET/CT Imaging. *Journal of Nuclear Medicine*, **48**, 196.

[32] Lee, T.-C., Zhang, R., Alessio, A.M., Fu, L., De Man, B. and Kinahan, P.E. (2017) Statistical Distributions of Ultra-Low Dose CT Sinograms and Their Fundamental *SPIE Medical Imaging*, Orlando, FL, 9 March 2017, pp. 101320N-101320N-7.

[33] Xia, T., Alessio, A.M., De Man, B., Manjeshwar, R., Asma, E. and Kinahan, P.E. (2012) Ultra-Low Dose CT Attenuation Correction for PET/CT. *Physics in Medicine & Biology*, **57**, 309-328. https://doi.org/10.1088/0031-9155/57/2/309

[34] Rui, X., Jin, Y., FitzGerald, P.F., Alessio, A., Kinahan, P. and Man, B.D. (2014) Optimal kVp Selection for Contrast CT Imaging Based on a Projection-Domain Method. *International Conference on Image Formation in X-Ray Computed Tomography*, Salt Lake, 22 June 2014, 173-177.

[35] Fu, L., Lee, T.-C., Kim, S.M., Alessio, A.M., Kinahan, P.E., Chang, Z., Sauer, K., Kalra, M.K. and De Man, B. (2017) Comparison between Pre-Log and Post-Log Statistical Models in Ultra-Low-Dose CT Reconstruction. *IEEE Transactions on Medical Imaging*, **36**, 707-720. https://doi.org/10.1109/TMI.2016.2627004

[36] Sun, M. and Star-Lack, J.M. (2010) Improved Scatter Correction Using Adaptive Scatter Kernel Superposition. *Physics in Medicine & Biology*, **55**, 6695-6720. https://doi.org/10.1088/0031-9155/55/22/007

[37] Gao, H., Fahrig, R., Bennett, N.R., Sun, M., Star-Lack, J. and Zhu, L. (2010) Scatter Correction Method for X-Ray CT Using Primary Modulation: Phantom Studies. *Medical Physics*, **37**, 934-946. https://doi.org/10.1118/1.3298014

[38] Zhang, Y., Yang, J., Zhang, L., Court, L.E., Balter, P.A. and Dong, L. (2013) Modeling Respiratory Motion for Reducing Motion Artifacts in 4D CT Images. *Medical Physics*, **40**, Article ID: 041716.

[39] Abdelnour, A.F., Nehmeh, S.A., Pan, T., Humm, J.L., Vernon, P., Schoder, H., Rosenzweig, K.E., Mageras, G.S., Yorke, E., Larson, S.M. and Erdi, Y.E. (2007) Phase and Amplitude Binning for 4D-CT Imaging. *Physics in Medicine & Biology*, **52**, 3515-3529. https://doi.org/10.1088/0031-9155/52/12/012

[40] Johnston, E., Diehn, M., Murphy, J.D., Loo, B.W. and Maxim, P.G. (2011) Reducing

4D CT Artifacts Using Optimized Sorting Based on Anatomic Similarity. *Medical Physics*, **38**, 2424-2429. https://doi.org/10.1118/1.3577601

[41] Schleyer, P.J., O'Doherty, M.J., Barrington, S.F. and Marsden, P.K. (2009) Retrospective Data-Driven Respiratory Gating for PET/CT. *Physics in Medicine & Biology*, **54**, 1935. https://doi.org/10.1088/0031-9155/54/7/005

[42] Bergner, F., Berkus, T., Oelhafen, M., Kunz, P., Pan, T. and Kachelriess, M. (2009) Autoadaptive Phase-Correlated (AAPC) reconstruction for 4D CBCT. *Medical Physics*, **36**, 5695-5706. https://doi.org/10.1118/1.3260919

[43] Shieh, C.-C., Kipritidis, J., O'Brien, R.T., Kuncic, Z. and Keall, P.J. (2014) Image Quality in Thoracic 4D Cone-Beam CT: A sensitivity Analysis of Respiratory Signal, Binning Method, Reconstruction Algorithm, and Projection Angular Spacing. *Medical Physics*, **41**, Article ID: 041912. https://doi.org/10.1118/1.4868510